Extensive observations of CO_2 carbon isotope content in and above a high-elevation subalpine forest

D. R. Bowling,[1] S. P. Burns,[2] T. J. Conway,[3] R. K. Monson,[2,4] and J. W. C. White[5]

Received 23 October 2004; revised 8 April 2005; accepted 14 July 2005; published 23 September 2005.

[1] The dynamics of forest-atmosphere CO_2 carbon isotope exchange were examined in a coniferous forest in Colorado, United States. Tunable diode laser absorption spectrometry provided extensive characterization of the carbon isotope content ($\delta^{13}C$) of CO_2. Observed patterns in $\delta^{13}C$ of forest air were associated with photosynthesis, respiration, and atmospheric boundary layer dynamics. Similar relationships between $\delta^{13}C$ and CO_2 were observed at all forest heights and confined to a relatively narrow envelope. Substantial variation was observed in the isotope ratio of nocturnal ecosystem respiration ($\delta^{13}C_R$, calculated from isotopic mixing lines). A systematic bias was identified when estimating $\delta^{13}C_R$ from data sets with small range in CO_2 in the samples, leading us to restrict analysis of $\delta^{13}C_R$ to periods with CO_2 range >40 μmol mol^{-1}. Values of $\delta^{13}C_R$ varied from −28.1 to −25.2‰, with variation from one night to the next as large as 1.7‰. A consistent difference was observed between $\delta^{13}C_R$ calculated near the forest floor (<2 m height) versus the upper canopy (5–11 m) on the same nights. $\delta^{13}C_R$ was more enriched in the upper canopy than near the ground on 34 of 43 nights, with a mean enrichment of 0.6‰ and a maximum of 2.3‰. A similar pattern was observed comparing $\delta^{13}C_R$ at night with the analogous quantity calculated during daytime, but only a few daytime periods met the 40 μmol mol^{-1} criterion. Comparisons between air samples measured (1) 10 m above the forest canopy, (2) 3 km away, and (3) within the convective boundary layer 125 km distant showed CO_2 differences between sites as large as 5–6 μmol mol^{-1} even at midday. These results suggest that attempts to use flask measurements at remote monitoring stations as a proxy for the air directly interacting with a vegetation canopy should be made with caution. However, our results also suggest that substantial information about biosphere-atmosphere isotopic exchange can be obtained by simultaneous examination of CO_2 and $\delta^{13}C$ at multiple spatial scales.

Citation: Bowling, D. R., S. P. Burns, T. J. Conway, R. K. Monson, and J. W. C. White (2005), Extensive observations of CO_2 carbon isotope content in and above a high-elevation subalpine forest, *Global Biogeochem. Cycles*, *19*, GB3023, doi:10.1029/2004GB002394.

1. Introduction

[2] Carbon sequestration by forests in complex mountain topography is difficult to quantify with eddy covariance measurements due to uncertainties in components of the turbulent and mean CO_2 fluxes [*Turnipseed et al.*, 2003, 2004] (also D. E. Anderson et al., Mean advective flux of CO_2 in a high elevation, subalpine forest during drainage flow conditions, submitted to *Agricultural Forest Meteorology*, 2005) (hereinafter referred to as Anderson et al., submitted manuscript, 2005). However, in many continental regions the majority of the regional carbon flux occurs in forests that occupy mountainous terrain [*Schimel et al.*, 2002]. This is especially true in the western United States, where lower productivity ecosystems tend to occupy low-elevation arid and semi-arid zones, and high rates of carbon sequestration are isolated to montane ecosystems along the Pacific Coast and in the Rocky Mountains. Relatively high rates of net primary production in these montane ecosystems are facilitated by high input of winter precipitation as snowfall. Ecosystems in complex terrain are likely responsible for a significant proportion of the land-atmosphere carbon exchange in North America [*Schimel et al.*, 2002] Thus it is important to develop observational approaches that will permit accurate quantification of regional carbon fluxes in mountainous landscapes.

[1]Department of Biology, University of Utah, Salt Lake City, Utah, USA.
[2]Department of Ecology and Evolutionary Biology, University of Colorado, Boulder, Colorado, USA.
[3]NOAA Climate Monitoring and Diagnostics Laboratory, Boulder, Colorado, USA.
[4]Also at Cooperative Institute for Research in Environmental Science, University of Colorado, Boulder, Colorado, USA.
[5]Institute of Arctic and Alpine Research (INSTAAR), University of Colorado, Boulder, Colorado, USA.

0886-6236/05/2004GB002394$12.00

[3] Eddy covariance measurements have added substantially to mechanistic understanding of carbon cycle processes in the last decade [e.g., *Baldocchi et al.*, 2001; *Law et al.*, 2002; *Valentini*, 2003; *Mencuccini et al.*, 2004]. However, uncertainties remain about some very basic carbon cycle questions. For example, it is unclear from eddy covariance studies whether ecosystem respiration [*Valentini et al.*, 2000] or gross primary production [*Janssens et al.*, 2001; *van Dijk and Dolman*, 2004] are responsible for observed latitudinal patterns in net ecosystem exchange of CO_2 (NEE) in Europe. Complementary methods for investigation of carbon cycle processes are needed. Independent constraints on eddy covariance estimates of the local carbon budgets of ecosystems can be developed from biometric surveys [*Barford et al.*, 2001; *Curtis et al.*, 2002], from evaluation of eddy flux data considering additional ecophysiological parameters such as light response [*Yi et al.*, 2004], by scaling up leaf, bole, and soil chamber measurements [*Law et al.*, 1999], with biophysical models [*Baldocchi and Meyers*, 1998], and using isotopic approaches.

[4] Stable isotopes are extensively used in contemporary carbon cycle research to elucidate biological and physical processes across spatial and temporal scales. Carbon isotopes have long been used to examine plant carbon-water relations [*Ehleringer et al.*, 1993] and are increasingly used to examine plant metabolic processes [*Ghashghaie et al.*, 2003], carbon allocation patterns [*Damesin and LeLarge*, 2003] and the physiological response of whole plants to environmental variation [*Pate and Arthur*, 1998; *Keitel et al.*, 2003]. At the regional and global scales, stable isotopes are used to examine ocean/land carbon sink strength [*Ciais et al.*, 1995; *Randerson et al.*, 2002; *Scholze et al.*, 2003], the influence of biological processes and fossil fuel use on the atmosphere [*Lloyd et al.*, 1996; *Bakwin et al.*, 1998; *Randerson et al.*, 2002; *Miller et al.*, 2003], and the ocean [*Gruber et al.*, 1999; *Quay et al.*, 2003].

[5] The present study focuses primarily on the scale of surface-layer eddy covariance flux towers (10^3–10^6 m^2). At the flux-tower (or ecosystem) scale, carbon isotopes are useful to partition NEE into the component fluxes of photosynthetic uptake and respiratory release [*Yakir and Wang*, 1996; *Bowling et al.*, 2001, 2003a; *Ogée et al.*, 2003, 2004; *Lai et al.*, 2003; *Knohl*, 2003] [see also *Schnyder et al.*, 2003]. Isotopes have been used extensively to investigate whole-ecosystem physiological processes through the application of isotopic mixing lines called Keeling plots [*Keeling*, 1958]. These mixing relationships provide the carbon isotope ratio ($\delta^{13}C$) of integrated nocturnal ecosystem respiration, denoted $\delta^{13}C_R$. $\delta^{13}C_R$ is controlled by environmental drivers in complex ways, but it is clear that mean annual precipitation [*Pataki et al.*, 2003], soil moisture [*Fessenden and Ehleringer*, 2003], humidity [*Ekblad and Högberg*, 2001; *Bowling et al.*, 2002], and temperature [*McDowell et al.*, 2004] are all involved. These and other studies demonstrate that examination of $\delta^{13}C_R$ is beginning to provide novel insight into ecosystem carbon cycling.

[6] Ecosystem-scale physiology studies that utilize CO_2 isotopes primarily focus on three related parameters: (1) $\delta^{13}C_R$, (2) the flux-weighted photosynthetic discrimination of the vegetation canopy (Δ_{canopy}), and (3) the isotopic difference between photosynthetic and respiratory fluxes (called isotopic disequilibrium). These quantities are important not only in ecosystem studies but also at the regional and global scales [*Randerson et al.*, 2002; *Miller et al.*, 2003; *Scholze et al.*, 2003]. An understanding of the magnitude and variability of these parameters in all biomes is critical to large-scale carbon balance studies such as those associated with the CarboEurope IP (http://www.carboeurope.org/) or North American Carbon Program (http://www.esig.ucar.edu/nacp/) efforts.

[7] This study was designed to shed light on the myriad factors controlling ecosystem-atmosphere isotopic exchange of CO_2, an analysis beyond the scope of a single paper. The influence of environmental drivers on $\delta^{13}C_R$, and the use of our isotopic data to partition NEE and investigate isotopic discrimination and disequilibria will be left to future papers. In this paper we describe the isotopic observations and place them in an ecological context with weather and flux data. We use these data to address three issues. First, does the natural isotopic composition of nocturnal respiration vary with height in a forest? Second, does $\delta^{13}C_R$ differ at night from the analogous quantity during the daytime? Third, how extensive is the local forest influence on CO_2 and $\delta^{13}C$ of CO_2 in the atmosphere, and can suitable proxy measurements for overlying air be made at other locations?

2. Methods

2.1. Study Location, Flux, and Meteorological Measurements

[8] This study was conducted in a subalpine coniferous forest (the Niwot Ridge AmeriFlux Tower site) in the Rocky Mountains of north-central Colorado, United States, during summer and fall 2003 (40.03°N, 105.55°W, 3050 m above sea level (masl)). Eddy covariance CO_2, H_2O, and energy fluxes and meteorology have been monitored continuously at this site since November 1998 [*Monson et al.*, 2002; *Turnipseed et al.*, 2002]. The site is located within 600 m of the C-1 long-term monitoring station which has a continuous weather record since 1951 [*Greenland*, 1989], and is part of the Niwot Ridge Long-Term Ecological Research program. The site is a ~100 year old mixed-species subalpine forest composed of *Abies lasiocarpa* (subalpine fir), *Picea engelmannii* (Engelmann spruce), and *Pinus contorta* (lodgepole pine). Canopy height during the study was 11–12 m.

2.2. Air Sampling at Ancillary Sites

[9] CO_2 and $\delta^{13}C$ measurements were made at two related locations, the tundra site and the aircraft site. The tundra site (historically called T-van [*Greenland*, 1989]) was located above treeline in the alpine tundra, roughly 3 km NW of the forest site at 40.05°N 105.58°W 3423 masl. Flask samples have been collected weekly at the tundra site as part of NOAA's Carbon Cycle Greenhouse Gases (CCGG) Cooperative Global Air Sampling Network for several decades (the site is called NWR by CCGG). The CO_2 record (measured in weekly flasks) began in 1968 [*Conway et al.*, 1994]. Stable isotopes of CO_2 in the flask samples have been measured since 1990 by the Stable Isotope Laboratory

Table 1. Comparison of Two Calibration Tanks Used in the Study, Arbitrary Example Tanks of Unrealistic Extreme Isotope Ratio (+100 and −100‰), and the Extreme Measured Values From Figure 4[a]

	CO_2, μmol mol^{-1}	$\delta^{13}C$, ‰	R	$^{12}CO_2$, μmol mol^{-1}	$^{13}CO_2$, μmol mol^{-1}
Tank 1	353.3	−8.2	0.011145	349.4	3.89
Tank 4	477.4	−8.9	0.011137	472.1	5.26
Arbitrary	350.0	+100.0	0.012361	345.7	4.27
Arbitrary	500.0	+100.0	0.012361	493.9	6.10
Arbitrary	350.0	−100.0	0.010113	346.5	3.50
Arbitrary	500.0	−100.0	0.010113	495.0	5.01
Measured	363.0	−7.6	0.011152	359.0	4.00
Measured	513.7	−12.9	0.011093	508.0	5.64

[a]Values for R, $^{12}CO_2$, and $^{13}CO_2$ are calculated from the others as described in section 2. Note that the variation in $^{12}CO_2$ and $^{13}CO_2$ are driven primarily by the wide range in total CO_2, not by $\delta^{13}C$.

at the University of Colorado's Institute of Arctic and Alpine Research [*Trolier et al.*, 1996].

[10] The aircraft site (40.90°N, 104.80°W, 1740 masl, called CAR by CCGG) was located near Carr, Colorado, roughly 125 km NNE of the Niwot Ridge sites. Aircraft flask samples have been collected from ground level (1740 m elevation) to up to 8000 m since 1992, and were collected approximately weekly during this study. Long-term data for these and other gases measured at the tundra and aircraft sites are available at http://www.cmdl.noaa.gov/ccgg/iadv/.

[11] In this paper we use measurements of CO_2 mole fraction ($[CO_2]$) and $\delta^{13}C$ in CO_2 in the flasks at the tundra and aircraft sites. Aircraft site data presented here are restricted to the altitude band 3500 to 4500 masl. For analytical details see *Thoning et al.* [1995] and *Trolier et al.* [1996]. Precision for $[CO_2]$ and $\delta^{13}C$ for the flasks is 0.1 μmol mol^{-1} and 0.01‰ [*King et al.*, 2002; *Allison et al.*, 2003].

2.3. Tunable Diode Laser Spectrometry

[12] Measurements of $[CO_2]$ and $\delta^{13}C$ in CO_2 were made at the forest site between July 2 and October 15 (days 184–289), 2003, using a tunable diode laser absorption spectrometer (TDL, model TGA100, Campbell Scientific, Inc., Logan, Utah). This instrument was described in detail by *Bowling et al.* [2003b]. Absorption lines used for the present study were 2293.881 and 2294.481 cm^{-1} for $^{12}CO_2$ and $^{13}CO_2$, respectively.

[13] A multi-inlet sampling manifold allowed automated sampling of multiple heights within the vegetation canopy and calibration gases. The TDL sampled nine heights within and above the canopy (0.1, 0.5, 1, 2, 5, 7, 9, 11, and 21.5 m) and four calibration gases every 6 min. All inlets were within or below the canopy except for 21.5 m, which was co-located with the eddy covariance flux instruments. The sample inlet air was pumped continuously through 0.18 mm critical flow orifices to maintain constant flow at 185 mL min^{-1}. Calibration gases only flowed when being measured. Switching between inlets occurred every 20 s; data from the first 10 s on each line were discarded to allow the plumbing to flush and pressure transients (<20 Pa) to dissipate in the TDL sample cell. Data from the last 10 s of each 20-s period were averaged to produce a measurement, with a single 10-s period per sampling height every 6 min. Pressure in the absorption cell during measurement was maintained at 2.1 kPa to minimize pressure broadening. Water vapor was removed before measurement using a Nafion counterflow system (PD 1000, Campbell Scientific, Inc., Logan, Utah).

[14] Calibration gases were CO_2-in-air mixtures that were filled with ambient air using a custom compressor system at the Stable Isotope Ratio Facility for Environmental Research, University of Utah (SIRFER). Above-ambient $[CO_2]$ in the tanks was obtained by addition of pure CO_2 with $\delta^{13}C$ near −10‰ prior to filling. A total of six tanks were used, ranging in CO_2 from 353.3 to 477.4 μmol mol^{-1} and $\delta^{13}C$ from −8.17 to −10.02‰. Since the TDL system measured $^{12}CO_2$ and $^{13}CO_2$ independently, it was not critical that the calibration gases differed in isotope ratio. This is illustrated conceptually by the values presented in Table 1. The large ranges in $^{12}CO_2$ and $^{13}CO_2$ observed in nature are driven primarily by the variation in $[CO_2]$, which is much greater than natural variation in $\delta^{13}C$ (even considering unrealistically large $\delta^{13}C$ variation of +100 and −100 ‰).

[15] $[CO_2]$ in calibration gases was propagated from four World Meteorological Organization (WMO)-traceable primary or secondary CO_2 standards via non-dispersive infrared gas analysis (NDIR, Licor 7000, Licor, Inc., Lincoln, Nebraska). The $\delta^{13}C$ of CO_2 in the calibration gases was measured relative to the VPDB scale using isotope ratio mass spectrometry (IRMS, Finnigan MAT DELTAplus, San Jose, California) at the SIRFER facility. Uncertainty for the calibration tank values was 0.16 μmol mol^{-1} and 0.05‰ (the maximum standard deviation of repeated measurements of all tanks on several different days before and after the field experiment).

[16] Field measurements of known calibration gases during the initial 2 months of the experiment are shown in Table 2. (Two initial tanks were replaced with tanks of similar value on days 254 and 262, and the other two original tanks were used for the entire experiment. Results for these tanks were similar to those in Table 2.) On the basis of an earlier study, we initially planned on using two calibration tanks [*Bowling et al.*, 2003b], reserving the other two as a reference point for data quality. However, the two-point calibration was deemed inadequate owing to unexplained diurnal variation in instrument response. Several calibration schemes were examined, each being applied on a 6-min basis to the data. For all calibrations, measured values of $[CO_2]$ and

Table 2. Performance of the TDL System on the Basis of Measurement of Known Calibration Gases[a]

	Tank 1 CO_2, μmol mol^{-1}	Tank 1 $\delta^{13}C$, ‰	Tank 2 CO_2, μmol mol^{-1}	Tank 2 $\delta^{13}C$, ‰	Tank 3, μmol mol^{-1}	Tank 3 $\delta^{13}C$, ‰	Tank 4 CO_2, μmol mol^{-1}	Tank 4 $\delta^{13}C$, ‰
Lab-measured "true" value	353.29	−8.17	379.62	−8.42	421.01	−10.02	477.40	−8.90
Uncertainty	0.16	0.05	0.16	0.05	0.16	0.05	0.16	0.05
Three-point mean	353.37	−8.20	379.72	−8.42	421.09	−10.00	477.64	−8.94
Three-point SD	0.15	0.16	0.07	0.13	0.09	0.14	0.40	0.22
Four-point mean	353.32	−8.18	379.72	−8.42	421.12	−10.00	477.47	−8.91
Four-point SD	0.09	0.10	0.05	0.09	0.07	0.10	0.33	0.10

[a]The four-point calibrations listed used all four tanks to establish a linear relationship between field-measured tank values and laboratory-measured (true) tank values, then report the corrected field-measured value for a particular tank based on this regression. Three-point calibrations are similar but avoid self calibration (e.g., Tanks 2, 3, and 4, but not Tank 1, were used to establish a regression, then Tank 1 was measured using this regression.) Data are means and standard deviations of 14,002 measurements of each tank.

$\delta^{13}C$ were used to calculate $^{12}CO_2$ and $^{13}CO_2$ mole fraction for each calibration tank. For this we used the equations $\delta^{13}C = 1000(R/R_{VPDB} - 1)$, $R = {}^{13}CO_2/{}^{12}CO_2$, and assumed R_{VPDB} (the $^{13}C/^{12}C$ ratio of the reference standard, VPDB) was 0.011237. The exact value of R_{VPDB} is not well described, and values in the literature differ by the equivalent of 5‰ [*Griffis et al.*, 2004]. However, since we report the $^{13}C/^{12}C$ ratio for our atmospheric sample values in $\delta^{13}C$ notation rather than $^{12}CO_2$ and $^{13}CO_2$ mole fractions, the assumed value has no bearing on the final results, canceling out upon returning to $\delta^{13}C$ notation. Final values for $[CO_2]$ in this paper are reported as $([12CO_2] + [13CO_2]) \times 100/99.526$ to account for other isotopes as described by *Bowling et al.* [2003b].

[17] To test the linearity and accuracy of the system over time, a three-point linear calibration scheme was applied. For each 6-min measurement cycle, the measured mole fractions of $^{12}CO_2$ and $^{13}CO_2$ in three calibration tanks were regressed versus the actual mole fractions (a separate regression for each isotopomer). This regression was applied to the fourth calibration tank, and the resulting value compared to the known value for the tank. The results of the three-point linear calibration shown in Table 2 demonstrate (1) there is no bias in $[CO_2]$ or $\delta^{13}C$ relative to the laboratory-measured (true) tank values and (2) with appropriate calibration the instrument can provide stable results over long time periods in the field. This calibration procedure demonstrates the linearity and accuracy of the TDL instrument over the well-calibrated range (353.3 to 477.4 μmol mol^{-1} CO_2 in this case). Subsequent experiments with the TDL in the lab have shown substantial nonlinearity outside this range (data not shown).

[18] Increasing the number of calibration tanks used in the regression decreased the residual of the measured values versus true values for the tanks (Table 2). We elected to use all four calibration tanks in our calibration scheme for best results. The probability distribution of the root mean square (RMS) error in measurement of four calibration tanks is shown in Figure 1. This figure includes all data during the experiment, both before (data in Table 2) and after calibration tank changes. The overall RMS residuals for the four tanks were always less than 0.3 μmol mol^{-1} and 0.25‰, and on average the errors were 0.06 μmol mol^{-1} and 0.06‰. The fact that the distributions appear to overlap numerically (with different units) is coincidence. Examination of Figure 1 led us to adopt arbitrary QA thresholds of 0.15 μmol mol^{-1} and 0.15‰. Any 6-min time period where the RMS residuals of the four tanks exceeded either threshold (with all four tanks involved in the RMS calculation) was deemed unacceptable and the data rejected. This resulted in exclusion of 7.3% of all available 6-minute data periods (n = 23,679 over the entire data set, a total of 180,221 isotope measurements of unknown air). Additional data were lost owing to power failure during thunderstorms, resulting in an overall data recovery which fully met the QA thresholds of 79.6% over 104.8 days.

[19] On the basis of these analyses, we conservatively estimate the precision for our TDL measurements during summer/fall 2003 to be 0.15 μmol mol^{-1} for CO_2 and 0.15‰ for $\delta^{13}C$. Figure 1 suggests that on average the performance might be substantially better, but establishing this with confidence would require known surveillance tanks that are treated as unknowns and measured repeatedly over long time periods. Table 2 suggests the accuracy of the

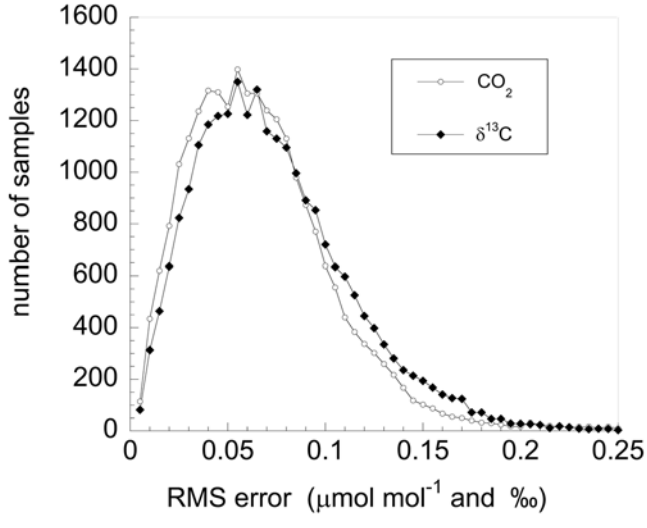

Figure 1. Distribution of the root mean square error in CO_2 and $\delta^{13}C$ measured by TDL on four calibration tanks. Each sample represents one measurement of each of the four tanks within a 6-min period. The entire 104-day data set is shown (n = 23,679 6-min periods). On the basis of this figure, data were rejected if the RMS error for CO_2 or $\delta^{13}C$ were greater than 0.15 μmol mol^{-1} or 0.15‰, respectively, resulting in rejection of 7.3% of available data.

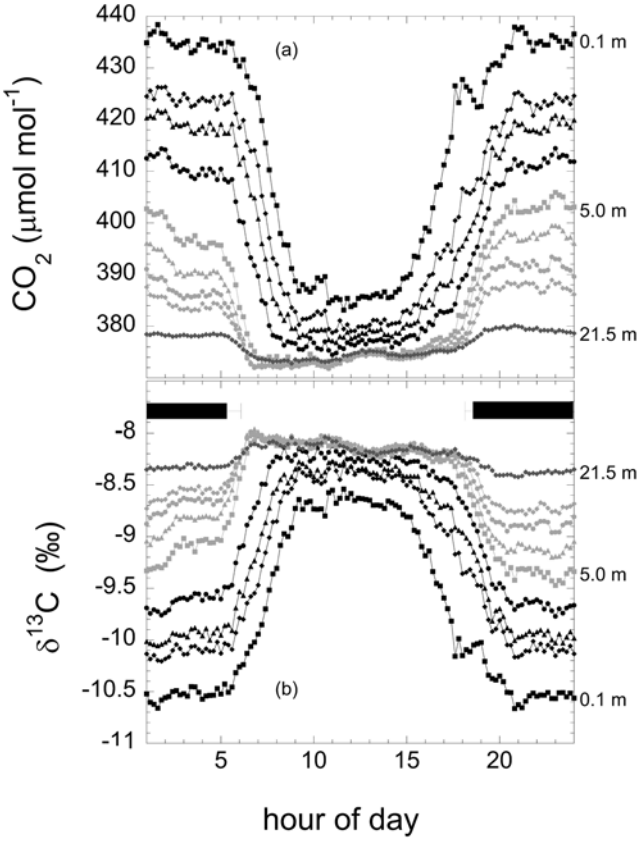

Figure 2. Average diel patterns in (a) CO_2 and (b) $\delta^{13}C$ at the forest site during the 104-day study period. All sampling heights are shown; only three are labeled as the heights change predictably in order. Night is indicated by the black bars, which are the mean (bar) and maximum (error bar) length of the dark period. Times are local standard time.

TDL measurements was indistinguishable from absolute at these precisions during our experiment.

2.4. Isotopic Mixing Lines

[20] The Keeling plot approach [*Keeling*, 1958] was used to determine $\delta^{13}C_R$. Assumptions associated with the Keeling approach have been discussed by *Pataki et al.* [2003], *Miller and Tans* [2003], and *Bowling et al.* [2003c, 2003d]. Outliers on individual plots were removed as described by *Bowling et al.* [2002]. Geometric mean regressions were used, and uncertainties are reported as the standard error of the intercept of an ordinary least squares regression. Keeling mixing lines were established for 6-hour periods from 9 pm to 3 am (night) or 9 am to 3 pm (day). We use $\delta^{13}C_R$ to denote Keeling plots constructed with nighttime data only, and $\delta^{13}C_{net}$ to denote Keeling plots with daytime data only. Preliminary analyses showed substantial differences between $\delta^{13}C_R$ measured near the ground or in the upper canopy. We initially tried to treat every sampling height as independent, but were often confronted with small CO_2 ranges in our samples. As we will demonstrate, small CO_2 ranges lead to large uncertainty in Keeling plot intercepts. Hence we selected those inlets near the ground (0.1, 0.5, 1.0, 2.0 m) as representative of soil processes and those in the upper canopy (5, 7, 9, and 11 m) as representative of foliar processes. Data from the four inlets in each category were grouped together on a single Keeling plot, with separate plots for the two categories.

3. Results and Discussion

3.1. CO_2 and Isotopic Dynamics

[21] The relative influences of photosynthesis, respiration, and atmospheric dynamics on the isotopic content of forest air can be illustrated with Figure 2. The panels show the mean diel patterns of $[CO_2]$ and $\delta^{13}C$ over the entire measurement period at various canopy heights. The CO_2 pattern within forests is now well-known [e.g., *Jarvis et al.*, 1997], but the isotopic pattern has not been well-established owing to limited measurement capability, particularly during the day [e.g., *Flanagan et al.*, 1996; *Bowling et al.*, 1999; *Ogée et al.*, 2003].

[22] Photosynthetic discrimination against the heavier $^{13}CO_2$ isotope leads to enrichment (defined as less negative $\delta^{13}C$) of the heavier isotope in forest air during the day when photosynthesis dominates. When plant organic compounds are later respired by leaf, bole, root, rhizosphere, or heterotrophic respiration, the CO_2 produced reflects that of organic matter, so respiration tends to make forest air less enriched in carbon-13 ($\delta^{13}C$ of air becomes more negative when respiration dominates). In our study, beginning in late afternoon, respiratory processes began to increase $[CO_2]$ at all heights, and this pattern continued throughout the night until sunrise, with highest $[CO_2]$ nearest the ground (Figure 2). Similarly, a consistent respiratory decrease in $\delta^{13}C$ was apparent as the night progressed, with most negative $\delta^{13}C$ near the ground.

[23] Following sunrise, atmospheric mixing increased owing to convective heating, photosynthesis was initiated, and $[CO_2]$ decreased while $\delta^{13}C$ became less negative. The rapid decrease in $[CO_2]$ from 0600–0900 local standard time (LST) reflects both atmospheric dynamics and photosynthesis. At 0600–0700 LST, the upper canopy and overlying air became well-mixed (Figure 2), with a minimum $[CO_2]$ and maximum $\delta^{13}C$ reached at roughly 0700 LST owing to photosynthetic removal of CO_2 and associated isotopic enrichment in the upper canopy before strong vertical mixing began. During this time, the upper canopy and air near the ground were somewhat decoupled on average. The large changes in $[CO_2]$ and $\delta^{13}C$ observed from night to day (between 0600 and 0900 LST) were primarily due to entrainment of overlying residual layer as the nocturnal boundary layer broke down and the daytime convective boundary layer grew. Diel $[CO_2]$ patterns similar to our observations have been observed as high as 500 m on tall towers that extend well above the surface layer [*Yi et al.*, 2000]. Note in Figure 2 that the influence of respiration is apparent in observed $[CO_2]$ and $\delta^{13}C$ even at midday, but only near the ground. This pattern likely leads to recycling of some fraction of soil-respired CO_2 [*Sternberg*, 1989] by plants in the understory and possibly upper canopy.

[24] The mean patterns shown in Figure 2 are illustrative of general patterns observed, but individual nights varied.

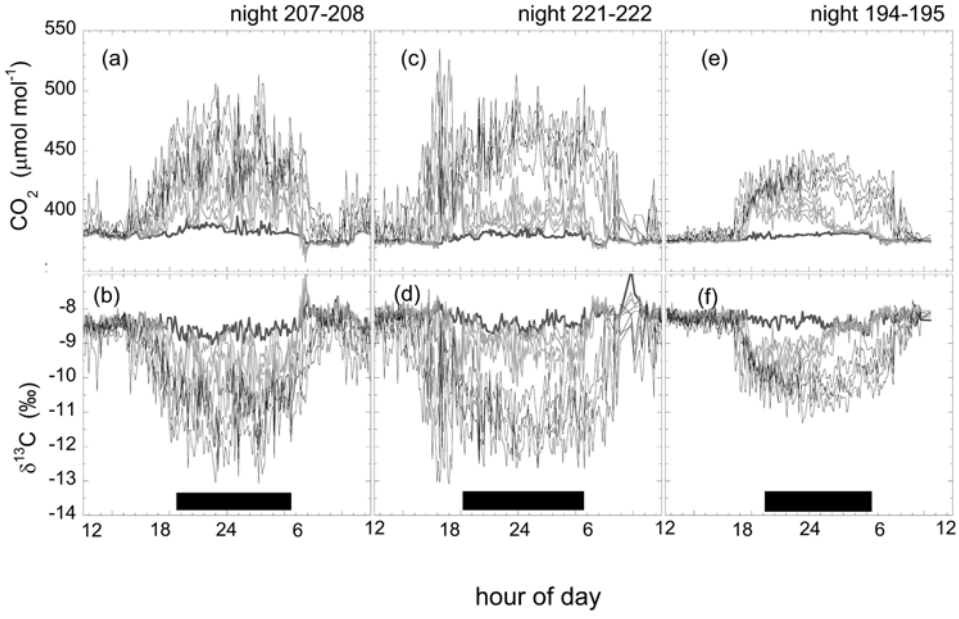

Figure 3. Patterns of CO_2 and $\delta^{13}C$ at all forest site measurement heights during selected nights (days 207–208, etc.). Sampling inlets near the ground (0.1, 0.5, 1.0, 2.0 m) are indicated with dark thin lines, those in the upper canopy (5, 7, 9, and 11 m) are shown as shaded thin lines, and above the canopy (21.5 m) a black thick line. Night is indicated by the black bars. Data shown are 6-min samples.

Three representative nights are shown in Figure 3. Night 207–208 showed consistent respiratory buildup of $[CO_2]$ and depletion of $\delta^{13}C$ at all heights, beginning 4 hours before sunset and persisting until 2 hours after sunrise. Early morning observations showed strong drawdown of $[CO_2]$ and photosynthetic enrichment of $\delta^{13}C$. Night 221–222 also involved strong $[CO_2]$ buildup near the ground, but the upper canopy was decoupled from this buildup for most of the night. The enriched period around 0900h may be an artifact – missing data (gaps in Figures 3c and 3d) during this time period were caused by large RMS errors on the calibration tanks (although the data shown on the figure did meet the QA thresholds). Night 194–195 initially showed strong buildup at all heights, but the buildup gradually decayed in the upper canopy, eventually reaching $[CO_2]$ and $\delta^{13}C$ values indistinguishable from those observed at 21.5 m. Similar patterns were observed with extensive vertical temperature profile measurements (data not shown), indicating the strong influence of atmospheric stability on our observations. These examples illustrate the potential complexities of atmospheric boundary layer dynamics in interpreting isotopic signals using Keeling plots.

3.2. Relationships Between $\delta^{13}C$ and CO_2

[25] The relationship between $\delta^{13}C$ and $[CO_2]$ is shown in Figure 4. A similar relationship was observed at all forest heights, but only three are shown on the plot for clarity. Measurements during July thru October were confined to a relatively narrow envelope on this graph. Higher $[CO_2]$ was always associated with more negative $\delta^{13}C$ owing to the tight biological coupling between them. Data are also shown for the tundra site for 1993, 1998, and 2003. The influence of the long-term trend in atmospheric CO_2 and

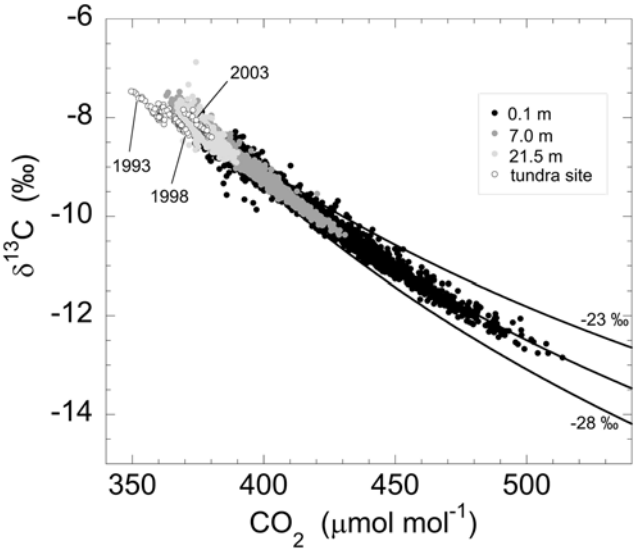

Figure 4. Relationship between $\delta^{13}C$ and CO_2 at the forest and tundra sites. The 30-min average data from three heights (0.1, 7.0, and 21.5 m) are shown for the 104-day study period. Weekly data from the tundra site are shown for 1993, 1998, and 2003 (year-round, not just summer). Lines represent Keeling mixing lines between an arbitrary background value (see text) and an isotopic source of −23 or −28‰, or the measured $\delta^{13}C_R$ signature of the 0.1 m data. The forest and tundra site data were collected by different laboratories, and we have not performed an intercomparison between groups.

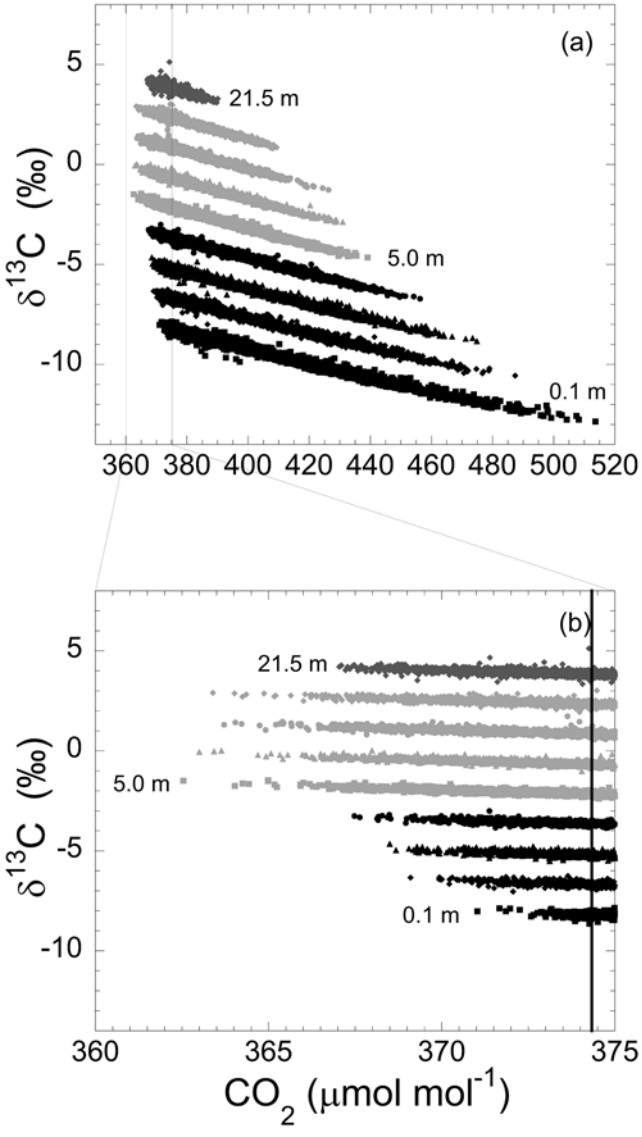

Figure 5. (a) Same as Figure 4, but data from all nine forest site heights are shown on the same plot. The $\delta^{13}C$ scale is only correct for the 0.1 m height; the others are shifted vertically by 1.5‰ each for clarity. Inlets near the ground are shown with black symbols, those in the upper canopy with light shaded symbols, and above the canopy with dark shaded symbols. (b) Same as Figure 5a, but the CO_2 scale has been expanded to show the low CO_2 range, which represents daytime periods and windy nights. The vertical line in b) represents the mean CO_2 observed at 21.5 m between 1000 and 1400 LST shown in Figure 2a.

$\delta^{13}C$ is apparent as a shift down and to the right from the earliest record to the latest. Variation within a year for the tundra data shows the seasonal cycles of CO_2 and $\delta^{13}C$. Comparison of the tundra and forest data illustrates the long-term (multiyear) global change trend and the short-term (hourly to several months) variability introduced by photosynthesis and respiration of the local forest.

[26] One may be tempted to assert that since the coupling between $\delta^{13}C$ and $[CO_2]$ appears tight, there is no unique information in $\delta^{13}C$. However, it is the variation within the envelope of Figure 4 that holds the most biologically relevant information. To provide a sense of biologically induced variation, theoretical Keeling-type mixing lines between an arbitrary background and a respiration source with $\delta^{13}C$ of -23 or -28‰ are shown in Figure 4. The background value for these mixing lines was taken as the mean of the tundra $[CO_2]$ (373.2 ± 2.4 μmol mol^{-1}, n = 13) and $\delta^{13}C$ (-8.02 ± 0.13‰, n = 13) data between days 182 and 290, 2003. Note that while the envelope containing the data appears relatively small on the graph, very large changes in a respiratory source signature (-23 to -28‰) still fall within this range. Plotting all data on the same graph obscures underlying biological variability (see Figure 7 in section 3.4). The overall Keeling mixing line for all data collected at the 0.1 m height is also shown (-25.73 ± 0.09‰, n = 1098). Note that variation in apparent respiratory source signature can also result from analytical or sampling errors [*Miller and Tans*, 2003].

[27] Similar data for all heights are shown in Figure 5a, offset for clarity. (When all heights are plotted together, they plot on top of each other as shown in Figure 4.) There was a clear difference in the amplitude of the observed diurnal variation at different heights. The highest $[CO_2]$ and most negative $\delta^{13}C$ measured were at the four inlets nearest the ground. $[CO_2]$ in the upper canopy did not exceed 440 μmol mol^{-1} at any time during the study. The low-$[CO_2]$ (daytime and windy nights) end of this figure is expanded in Figure 5b. The influence of photosynthetic drawdown of $[CO_2]$ within the upper canopy is apparent, particularly when compared to the 21.5 m height (vertical line in Figure 5b) which was 10 m above canopy top. These data provide some justification for our separation of heights into a component near the ground (dark symbols) and one in the upper canopy (light symbols) as indicative of soil and foliar processes, respectively.

[28] Figures 4 and 5 suggest that measurements of $[CO_2]$ may be used to provide a rough estimate of the variation in $\delta^{13}C$ that might be observed at a given height within a forest, provided an appropriate local mixing line is established for that forest. This could in principle be done with fewer measurements than we have used. Overall, we observed $[CO_2]$ variation from 362.5 to 513.7 μmol mol^{-1} and isotopic variation from -7.47 to -12.85‰. These ranges provide a rough estimate for isotopic variation in a C_3 ecosystem as 5.4‰/151 μmol mol^{-1} or 0.04‰ for each 1 μmol mol^{-1} change in CO_2. This relationship is not expected to remain constant, but the overall magnitude of $\delta^{13}C$ variation and CO_2 variation are generally correlated.

[29] This correlation is a useful proxy for determining isotopic instrument requirements at other sites. For example, if a tunable diode laser were to be designed for eddy covariance measurements of ^{13}C isofluxes, what isotopic signals would need to be measured, and with what precision and accuracy? The maximum range of CO_2 observed at the eddy flux height (21.5 m) during our study was 367.0 to 390.0 μmol mol^{-1} (day and night included), a range of only 33 μmol mol^{-1}. Hence we could predict that the maximum

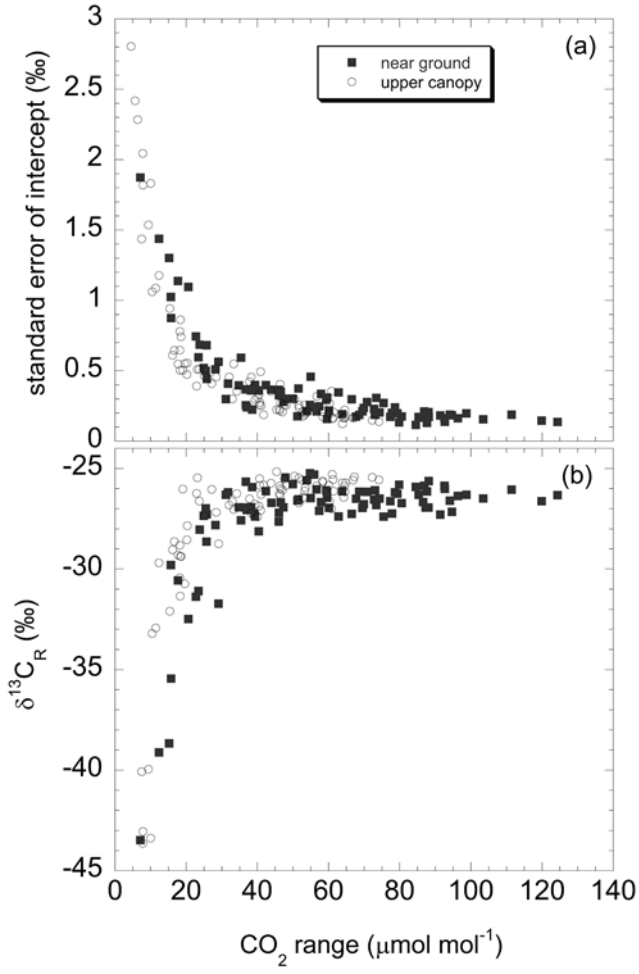

Figure 6. (a) Standard error of the Keeling plot intercept (for ordinary least squares regression, nocturnal data only) versus range of CO_2 in the data used for the regression [see also *Pataki et al.*, 2003]. (b) Keeling plot intercept (for geometric mean regression, nocturnal data only) versus range of CO_2. Data are shown for inlets near the ground (squares) and in the upper canopy (circles) separately.

isotopic range that might be observed at this height would be 33 × 0.04 or 1.32‰ (see Figure 4), and during a given 30-min flux measurement period it would be much smaller. An isotopic analyzer with precision of 0.05‰ would have at best a signal-to-noise ratio (SNR) of 26 in this case. Sites with substantially lower CO_2 flux magnitudes would have more serious constraints. If isotope errors are randomly distributed and not correlated with vertical wind velocity, the uncertainty in isoflux may be less sensitive to SNR than the above indicates. Regardless, eddy covariance measurements of isotopic fluxes will benefit from development of fast-response isotopic analyzers with higher precision than currently available.

3.3. Uncertainties in $\delta^{13}C_R$

[30] *Pataki et al.* [2003] showed that the uncertainty in determination of $\delta^{13}C_R$ using the Keeling-plot approach was increased when only a small measured $[CO_2]$ range was available. We observed the same pattern with somewhat less noise in our data (Figure 6a). However, we discovered a major systematic bias in $\delta^{13}C_R$ with small $[CO_2]$ ranges (Figure 6b), and this occurred with either inlet category (near ground or upper canopy). In general, small $[CO_2]$ ranges were always associated with erroneously negative $\delta^{13}C_R$. This is not an artifact of the TDL measurements, as it can be reproduced by taking a straight line and randomly assigning error to $\delta^{13}C$ and $[CO_2]$, then sub-sampling the data to obtain small $[CO_2]$ ranges. The problem is also apparent with another (non-Keeling) method of computing $\delta^{13}C_R$ proposed by *Miller and Tans* [2003]. We will address this issue in a subsequent paper (J. Zobitz et al., Sensitivity analysis and quantification of uncertainty for isotopic mixing relationships in carbon cycle research, submitted to *Agricultural and Forest Meteorology*, 2005). Here we restrict our interpretation of Keeling-plot analyses to periods when at least a 40 μmol mol^{-1} range in $[CO_2]$ was observed.

3.4. Environmental Drivers, Fluxes, and $\delta^{13}C_R$

[31] Weather and flux data for 2003 at the Niwot Ridge AmeriFlux forest are shown in Figure 7, to illustrate how our isotopic sampling period (within the vertical lines) compared to other time periods of the year. Significant snow cover exists at the site in the winter, and cold temperatures prevent net carbon uptake in the evergreen forest until snowmelt begins [*Monson et al.*, 2002]. Snowmelt occurred in late spring (roughly day 130 in 2003, Figures 7a and 7b) and the timing is a primary control on total annual carbon gain. Earlier snowmelt at Niwot Ridge can lead to lower annual carbon gain [*Monson et al.*, 2002] due to subsequent summer water limitation, in contrast with deciduous forest systems [e.g., *Goulden et al.*, 1996]. In 2003, the major period of carbon uptake and abundant soil moisture preceded the isotope measurements (Figures 7b and 7d). Several summer episodes with net daily respiration were observed, and the isotope measurements ended just as the transition to net respiration occurred and air and soil temperatures returned to freezing (Figures 7a and 7d). A transition from maximal to low evapotranspiration rates was captured during the measurement period (Figure 7e), as were some of the highest and lowest vapor pressure deficit (VPD) episodes of the year (Figure 7c). Summer thunderstorms caused variation in soil moisture but the magnitude was small relative to the major seasonal change associated with snowmelt (Figure 7b).

[32] We observed variation in the isotopic composition of respiration from −28.1 to −25.2‰ (Figure 7f). This is a fairly narrow range compared to reports of variability from other coniferous forests (overall range of 8 to 9‰ [*Bowling et al.*, 2002; *Lai et al.*, 2005; *McDowell et al.*, 2004; *Mortazavi et al.*, 2005]), although variation during the summer tends to be less than overall variation over an annual period [*Lai et al.*, 2005]. However, the possible influence of the systematic bias shown in Figure 6b is uncertain in these studies, particularly in winter when small CO_2 ranges are common. Only periods with $[CO_2]$ ranges >40 μmol mol^{-1} (61 nights) are shown in Figure 7f.

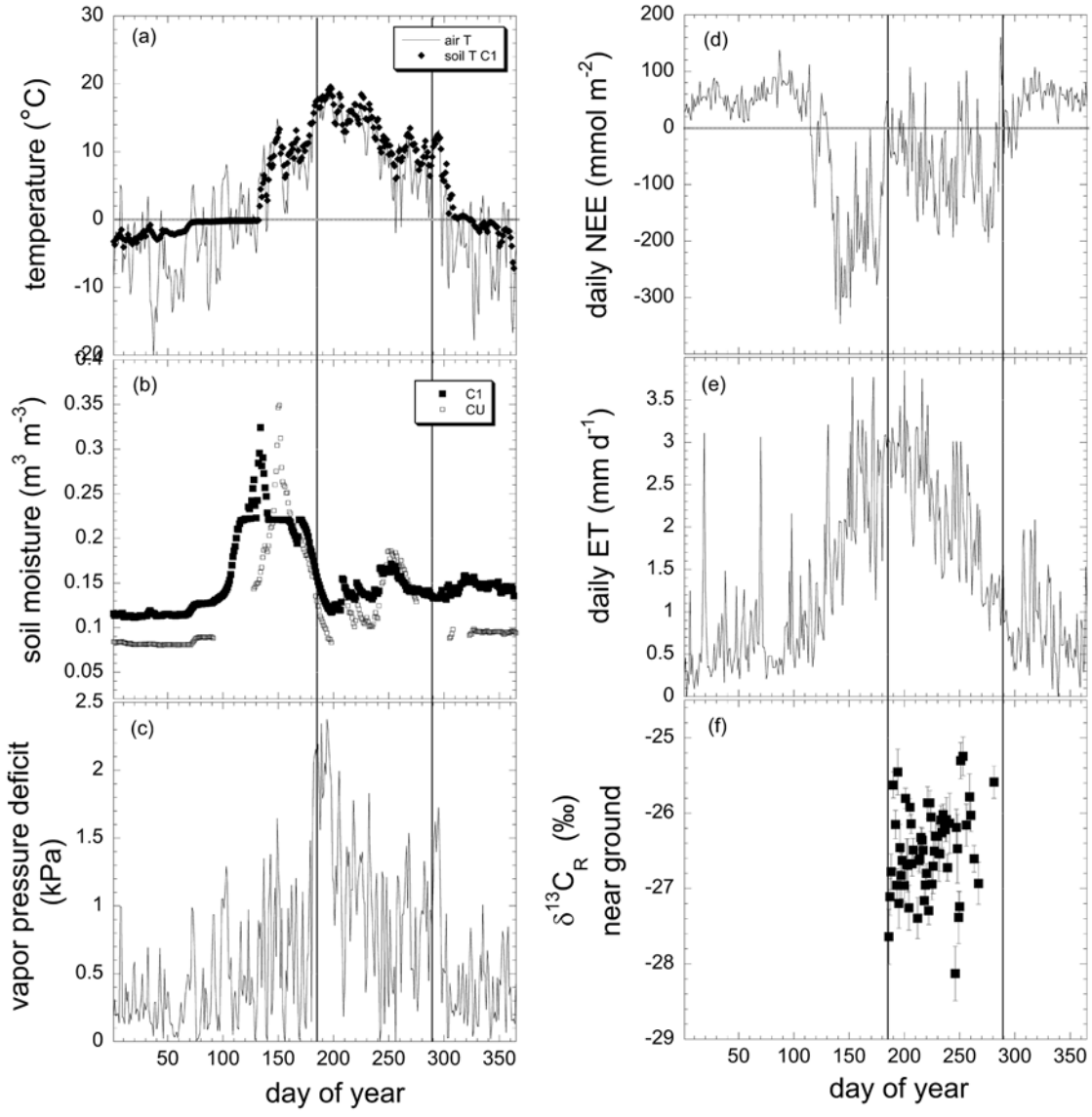

Figure 7. Annual weather, flux, and isotope data for 2003 at the forest site. (a) Air and soil temperature, (b) soil moisture at two locations within the tower area (C1 and CU), (c) vapor pressure deficit of air, (d) total daily net ecosystem exchange of CO_2, (e) total daily evapotranspiration, and (f) nocturnal $\delta^{13}C_R$ from the inlets near the ground with CO_2 ranges >40 μmol mol^{-1}. Vertical lines show the isotopic measurement period.

[33] There has been considerable focus recently on linkages between environmental factors and $\delta^{13}C_R$. A relation between precipitation and $\delta^{13}C_R$ has emerged as a general ecosystem pattern; mean annual precipitation (MAP) is a primary driver of the *mean* $\delta^{13}C_R$ within a given C_3 ecosystem, in temperate coniferous and deciduous forests, boreal forests, tropical forests, and grasslands [*Bowling et al.*, 2002; *Pataki et al.*, 2003, Figure 10]. The average $\delta^{13}C_R$ observed at Niwot Ridge during summer 2003 was −26.5 ± 0.6‰ (mean ± SD, n = 61, Figure 7f), which at 800 mm MAP follows the *Pataki et al.* [2003] prediction.

[34] In the present study we observed large variation in soil moisture and VPD (Figures 7b and 7c), factors which are known to influence $\delta^{13}C_R$ [e.g., *Lai et al.*, 2005; *Bowling et al.*, 2002]. Initial analysis suggests there was not a dominating link between VPD and $\delta^{13}C_R$ at Niwot Ridge during summer 2003 (Figures 7c and 7f). The influence of environmental drivers on $\delta^{13}C_R$ in the present study will be examined in detail in a future paper.

3.5. The $\delta^{13}C_R$ and Sampling Height Within the Forest

[35] To date, most studies of the isotopic composition of ecosystem respiration combine all sampling heights within a forest together for a single Keeling plot, rather than treating heights independently [e.g., *Bowling et al.*, 2002]. Combining data from many heights has the distinct advantage of increasing the $[CO_2]$ range of samples collected and thus minimizes uncertainty of the intercept [*Pataki et al.*, 2003]

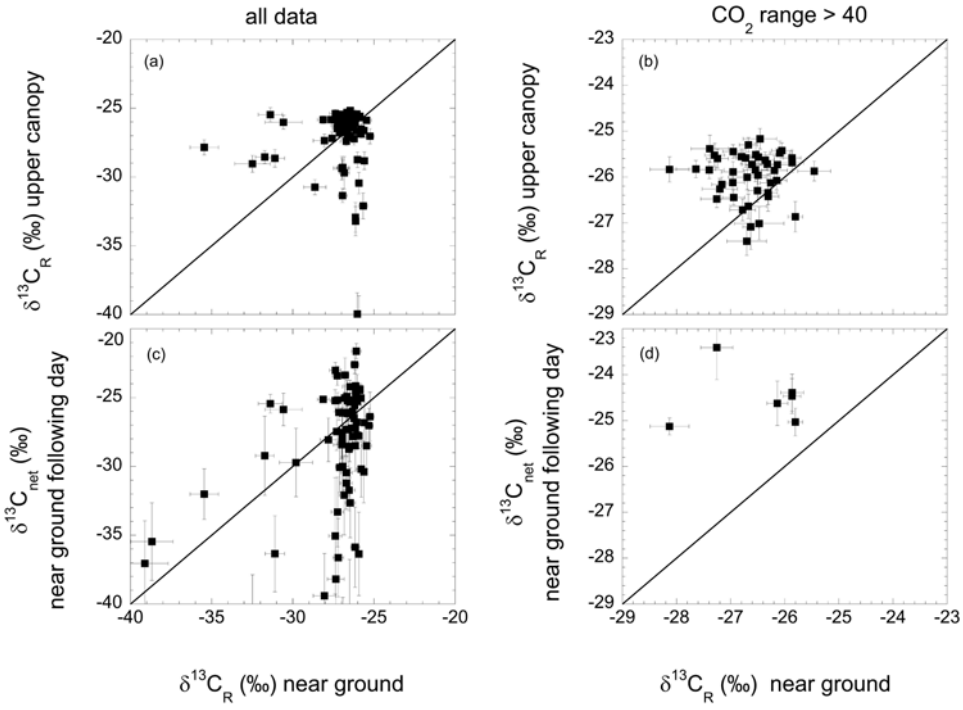

Figure 8. (a) The $\delta^{13}C_R$ calculated using the upper canopy inlets (5, 7, 9, and 11 m) versus the inlets near the ground (0.1, 0.5, 1.0, 2.0 m) for the same 6-hour nocturnal periods centered on midnight. All available data are shown. (b) Same as Figure 8a, but only those data with CO_2 ranges > 40 μmol mol^{-1} are shown. (c) The $\delta^{13}C_R$ calculated using the inlets near the ground (0.1, 0.5, 1.0, 2.0 m) for 6-hour night periods centered on midnight (abscissa, same as in Figure 8a) or $\delta^{13}C_{net}$ during the 6-hour daytime period centered on noon the next day (ordinate). All available data are shown. (d) Same as Figure 8c but only those data with CO_2 ranges > 40 μmol mol^{-1} are shown. Error bars are the standard error of the ordinary least squares intercept, and 1:1 lines are shown in each panel. Note that the left and right panels differ in scale.

and the bias problem in Figure 6b. However, different biota will influence the composition of air at different heights (Figure 2), and the surface footprint of concentration (and isotope) measurements is strongly dependent on height [*Schmid*, 1997; *Raupach*, 2001].

[36] Although limited to a single night, the study of *Ogée et al.* [2003] convincingly demonstrated that $\delta^{13}C_R$ in a *Pinus pinaster* forest was more enriched in the canopy than nearer the ground by 4–5‰. Our study provides additional evidence for an isotopic difference in the soil and foliar components of nighttime respiration. $\delta^{13}C_R$ for our inlets near the ground and in the upper canopy, calculated during the same nocturnal periods, are compared in (the misleading) Figure 8a. In general, samples collected within the canopy will have a smaller [CO_2] range than those near the ground (Figure 5), and smaller [CO_2] ranges lead to a systematic negative bias in $\delta^{13}C_R$ (Figure 6). This means that, without knowledge of the bias, one would erroneously find more negative $\delta^{13}C_R$ in the canopy on average. When only those nights with ranges in excess of 40 μmol mol^{-1} at both locations were considered (Figure 6), we observed a clear enrichment in the canopy relative to the ground (Figure 8b and Table 3). This opposes the prediction we would expect due to the bias (more depleted in the canopy) and is consistent with *Ogée et al.* [2003]. The pattern appears robust when the CO_2 range allowed for comparison is restricted so that the canopy and near-ground ranges are similar (Table 3). *Klumpp et al.* [2005] have shown with laboratory studies that shoot respiration is generally more enriched than root respiration in sunflower, alfalfa, and ryegrass. Our observations provide additional evidence that this may be a general phenomenon.

[37] If foliar respiration is in general more enriched than soil respiration, patterns of carbon allocation and carbon residence time within forests, and their independent linkages to environmental variation (such as VPD or radiation) may be examined using stable isotopes. This is particularly true for the autotrophic/rhizospheric component that appears to be tightly linked to environmental variation [*Fitter et al.*, 1999; *Gessler et al.*, 2001; *Ekblad and Högberg*, 2001; *Bowling et al.*, 2002; *Keitel et al.*, 2003; *Knohl et al.*, 2005].

[38] This is potentially an important finding, but more research is necessary for at least three reasons. First, the terrain at the Niwot Ridge AmeriFlux site is complex for an eddy flux tower, with a consistent 5°–7° slope and large mountains 8 km to the west. The terrain leads to mesoscale flow patterns including valley/mountain flows, mountain lee-side waves, and gravity waves [*Turnipseed et al.*, 2004], as well as influences on local fluxes [*Turnipseed et al.*, 2003]. Most relevant to this study are katabatic

Table 3. Mean Difference in $\delta^{13}C_R$ in the Upper Canopy ($\delta^{13}C_{R\text{-}UC}$) and $\delta^{13}C_R$ Near the Ground ($\delta^{13}C_{R\text{-}NG}$) From Figure 8b, Broken Down as a Function of CO_2 Range[a]

Minimum CO_2 Range, μmol mol^{-1}	Maximum CO_2 Range, μmol mol^{-1}	Mean Difference, ‰	SD of Difference, ‰	n
40	50	0.72	1.09	7
40	60	0.81	0.97	9
40	70	0.66	0.86	18
40	80	0.63	0.84	26
40	90	0.65	0.8	32
40	100	0.67	0.77	38
40	110	0.68	0.76	39
40	120	0.65	0.76	41
40	130	0.65	0.75	42
40	140	0.65	0.75	42
40	150	0.66	0.75	43

[a]For example, there were seven time periods (n) where both $\delta^{13}C_{R\text{-}UC}$ and $\delta^{13}C_{R\text{-}NG}$ were calculated from samples with CO_2 ranges between 40 and 50 μmol mol^{-1}, and the average difference ($\delta^{13}C_{R\text{-}UC}$ - $\delta^{13}C_{R\text{-}NG}$) was 0.72‰. SD is standard deviation.

(drainage) flow patterns which transport CO_2 via advection [*Turnipseed et al.*, 2003; Anderson et al., submitted manuscript, 2005]. Katabatic flow patterns can develop on much shallower slopes [*Aubinet et al.*, 2003; *Staebler and Fitzjarrald*, 2004]. While the slope at the forest site is steeper than most eddy flux sites, it is shallower than the vast majority of mountainous terrain. If different heights within the canopy are differentially influenced by drainage flow patterns, then the pattern in Figure 8b may be due to atmospheric transport phenomena and not biological processes. At this stage we do not know which is more important.

[39] Second, the observation of enriched foliar respiratory $\delta^{13}C$ relative to that of soil respiration must be reconciled with other studies, some with contrasting results. Several studies have shown that leaf respiration is enriched relative to leaf starch and sucrose [*Ghashghaie et al.*, 2003]. The apparent fractionation associated with dark respiration is thought to be due to non-uniform isotope distribution within molecules or fractionation during the pyruvate dehydrogenase reaction [*Ghashghaie et al.*, 2003]. While consistent with our observations, little is known about how this fractionation might influence carbon exported from the leaf. *Damesin and LeLarge* [2003], however, have shown that stem respiration is depleted relative to starch, and suggested two fractionations were important – one during sugar export from leaves and one during stem respiration.

[40] Third, the potential role of symbionts and decomposers in the soil respiration flux is also complex. Some fungi fractionate during uptake of sugars [*Henn and Chapela*, 2000], and decomposing fungi can be enriched by 4‰ relative to their substrates in wood [*Gleixner et al.*, 1993]. An examination of $\delta^{13}C$ of several plant materials relative to the CO_2 evolved during their decomposition by microbes showed that respired CO_2 was initially depleted relative to solid substrates, then gradually became more enriched [*Fernandez et al.*, 2003]. Other researchers have found similarities between $\delta^{13}C$ of respired CO_2 and soil organic matter but noted that microbial biomass was enriched and microbial respiration was depleted relative to SOM, effectively balancing out important isotopic variation [*Santruckova et al.*, 2000]. Further, soil organic matter is consistently enriched relative to plant tissues [e.g., *Balesdent et al.*, 1993]. Considerably more work is necessary to establish the controls on the isotopic composition of respiration from ecosystem components.

3.6. The $\delta^{13}C_R$ at Night Versus the Day

[41] A long-standing question in studies of $\delta^{13}C_R$ is whether the isotopic signature of ecosystem respiration differs at night versus during the day [e.g., *Buchmann et al.*, 1997]. Current attempts to use CO_2 isofluxes to partition NEE into respiration and photosynthesis fluxes [*Yakir and Wang*, 1996; *Bowling et al.*, 2001, 2003a; *Ogée et al.*, 2003; *Knohl*, 2003] assume the isotopic signature of respiration does not change on a diel basis. Since the one-way fluxes obtained from isotopic partitioning are dependent on the actual disequilibrium between the true photosynthetic and respiratory fluxes [*Ogée et al.*, 2004], the partitioning results are directly dependent on this assumption. $\delta^{13}C_R$ calculated near the ground at night is compared with $\delta^{13}C_{net}$ the following day in Figures 8c and 8d. As with Figure 8a, the systematic bias of Figure 6b led us to examine only those periods with CO_2 ranges above 40 μmol mol^{-1} (Figure 8d). Unfortunately only a few days met this criterion, so the comparison represents unusually stable daytime conditions. All days that did meet the criterion showed enrichment during the day relative to at night (Figure 8d). This could be caused by (1) changes in the isotopic content of total ecosystem or soil respiration, (2) photosynthetic influences on the mixing relationships, or (3) anabatic (uphill) flow during the day. Photochemistry experiments at the site have shown that urban air from the Denver-Boulder metropolitan area to the east can be transported via easterly (uphill) winds during the daytime in the summer at Niwot Ridge. This phenomenon occurs as the mixed-layer over the Great Plains to the east grows deep enough to encompass the site [*Parrish et al.*, 1990, 1991]. We are uncertain how these flow patterns might influence our results. Long-term measurements, as well as measurements of the isotopic content of component fluxes (soil versus foliage) are needed to examine these processes further.

3.7. Local and Non-Local Influences on CO_2 and $\delta^{13}C$

[42] A comparison of midday measurements made at the forest, tundra, and aircraft sites is shown in Figure 9. All available flask data are included for the tundra and aircraft

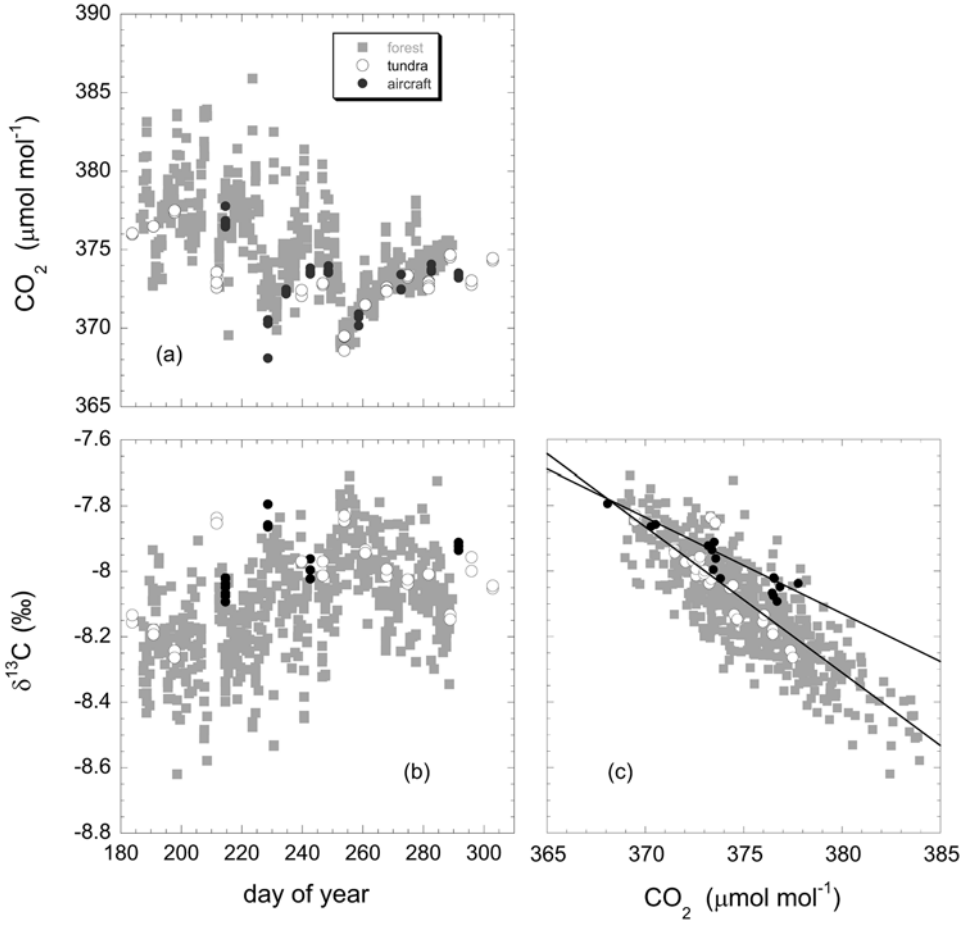

Figure 9. (a) Time series of CO_2 measured at three spatial scales during summer 2003. Forest data were collected at 21.5 m at midday (1200 to 1500) at 3050 m elevation. Tundra (3423 m) and aircraft data (3500 to 4500 masl) were collected approximately weekly. Data points represent individual flask measurements. (b) Same as Figure 9a but for $\delta^{13}C$. (c) The $\delta^{13}C$ versus CO_2 for the data in figures 9a and 9b. Regression lines shown are for the forest ($y = -0.044x + 8.56$, $r^2 = 0.72$, $n = 552$) and aircraft ($y = -0.029x + 3.04$, $r^2 = 0.88$, $n = 16$) sites; the tundra site line ($y = -0.052x + 11.26$, $r^2 = 0.79$, $n = 27$) is not shown. The forest and tundra/aircraft data were collected by different laboratories, and we have not performed an intercomparison between groups.

sites, so measured variability is represented in Figure 9. Forest site measurements (made 10 m above the canopy) sometimes differed substantially from the nearby (tundra, 3 km) and more distant (aircraft, 125 km) sites even at midday. Synoptic-scale changes in CO_2 and $\delta^{13}C$ were apparent, and correlated with changes in atmospheric pressure (pressure data not shown). Abrupt CO_2 changes of similar magnitude have been observed during the passage of storm fronts in Wisconsin [*Hurwitz et al.*, 2004]. Because the tundra and aircraft sites were characterized only weekly, the relative influences of the local and non-local atmosphere on the forest site remain unclear. In any case, the atmosphere that a photosynthesizing or respiring forest interacts with involves both non-local and local effects. Forest air reflects the sum of influences at these varying spatial scales. As we demonstrate below, approaches which use background data collected at a remote monitoring station as the ''input'' air to a forest should be used cautiously. This practice has so far been necessary in many biosphere-atmosphere isotopic exchange studies [e.g., *Buchmann et al.*, 1998; *Lai et al.*, 2004] due to a lack of available data. We argue that emphasis should be placed on characterization of CO_2 and $\delta^{13}C$ of air at multiple spatial and temporal scales when possible.

[43] One of the most important parameters in biosphere-atmosphere isotope exchange studies is the flux-weighted photosynthetic discrimination of the vegetation canopy (Δ_{canopy}) or the analogous quantity at larger scales. At present, this quantity is poorly constrained by measurements. Ecosystem discrimination (Δ_e [*Buchmann et al.*, 1997]) is often used as a proxy for Δ_{canopy}. However, this definition primarily reflects the isotopic difference between $\delta^{13}C$ of CO_2 in the free troposphere (which is hard to define) and $\delta^{13}C_R$, a nocturnal-respiration-based measurement. A respiratory definition of ecosystem discrimination as a proxy for a photosynthetic process is likely to miss important aspects of true photosynthetic discrimination, and prevents separate examination of photosynthetic discrimi-

nation and the disequilibrium between respiration and photosynthesis. Both parameters are critical to local and regional carbon balance studies.

[44] Limited attempts to examine Δ_{canopy} have been made based on measurements of air during the daytime. *Bowling et al.* [2001] and *Knohl* [2003] used a big-leaf approach based on latent heat flux measurements, inverting the Penman-Monteith equation to obtain a canopy conductance and ultimately $\Delta_{canopy.}$ A second approach proposed by *Lloyd et al.* [1996] involves examination of CO_2 and $\delta^{13}C$ in updrafts and downdrafts in an analogy with leaf-level "online" isotope discrimination. Both methods have serious problems in some situations. Multilayer or big-leaf biophysical canopy process modeling approaches have yielded reasonable estimates of Δ_{canopy} [*Baldocchi and Bowling*, 2003; *Ogée et al.*, 2003; *Lai et al.*, 2003]. However, at the ecosystem scale, the measurement-based (15–17‰) and model-based (20–21‰) estimates differ. These differences are more than sufficient to significantly alter the magnitude of the terrestrial carbon sink resulting from large-scale atmospheric studies [*Randerson et al.*, 2002; *Scholze et al.*, 2003]. Methods are needed to provide direct measurements of Δ_{canopy} at the ecosystem and regional scales to provide confidence in any regional carbon balance assessment using stable carbon isotopes.

[45] *Lai et al.* [2004] recently proposed a useful method to estimate Δ_{canopy}. Their approach involves rearranging the Keeling mixing-line equation [*Keeling*, 1958] so that a time-varying "background" atmosphere can be specified, which has proven useful at regional and global scales [*Bakwin et al.*, 1998; *Miller and Tans*, 2003; *Miller et al.*, 2003]. The appropriate background atmosphere is unfortunately hard to define, yet is very important. *Lai et al.* [2004] discuss this difficulty in detail and provide a sensitivity analysis to several background estimates.

[46] *Lai et al.* [2005] compared GLOBALVIEW database estimates of CO_2 and $\delta^{13}C$ with local midday measurements at the Wind River, Harvard and Howland Forest AmeriFlux sites. These data were used to determine an isotopic signature of net ecosystem CO_2 exchange, and combined with measured $\delta^{13}C_R$, local eddy flux estimates of NEE, and NEE-derived respiration and photosynthesis fluxes to determine Δ_{canopy}, following the *Lai et al.* [2004] method. The sites were at similar latitudes but several thousand km apart. The GLOBALVIEW product provides only time-varying zonal means of marine boundary layer measurements of CO_2 (or $\delta^{13}C$ from *Lai et al.* [2005]) at particular latitudes. Hence the exact description of the background atmosphere for this approach is a challenge, particularly if short-term variation in Δ_{canopy} is desired. For example, consider Figure 9. The relationship between midday $\delta^{13}C$ and CO_2 at all three scales is shown in Figure 9c. Similar mixing relationships (slopes) were observed at the forest and tundra sites, but the aircraft site showed a shallower slope. The shallower slope might reflect either a contribution of C_4 photosynthesis (perhaps from crops) or a lower C_3 discrimination (perhaps from water stress) in the agricultural areas and short-grass prairie to the east. What would be the appropriate background to use with the *Lai et al.* [2004] approach for the Niwot Ridge forest site: the tundra site, the aircraft site, or a zonal mean? How might estimates of Δ_{canopy} differ on the basis of these scales, and is there useful information that can be extracted from the differences? Synoptic changes in CO_2 or $\delta^{13}C$ such as those shown in Figure 9 or the work of *Hurwitz et al.* [2004] provide an additional challenge for short-term studies.

[47] The important conceptual advances of *Lai et al.* [2004, 2005] are promising but presently hampered by a lack of measurements. These studies and ours strongly underscore the need for intensive isotopic sampling at flux sites and much better characterization of the atmospheric background, at multiple spatial and temporal scales.

4. Conclusions

[48] The carbon isotope content of CO_2 in forest air was intensively examined over a three-month period at the Niwot Ridge AmeriFlux site in summer and fall 2003. Photosynthetic, respiratory, and atmospheric processes contributed to observed isotopic patterns. A systematic bias was found when estimating $\delta^{13}C_R$ from data sets with small CO_2 range in the samples. A difference in $\delta^{13}C$ of foliar and soil respiration was identified, with the former generally more enriched in ^{13}C than the latter. Daytime Keeling plots tended to be more enriched than those the previous night near the forest floor. Finally, relationships between $\delta^{13}C$ and CO_2 at three spatial scales showed important differences that highlight the need for future work examining biosphere-atmosphere isotopic exchange patterns at a variety of spatial and temporal scales.

[49] **Acknowledgment.** We thank S. Sargent for help in the field and many thoughtful discussions about TDL spectrometry, and J. Miller for discussions about large-scale atmospheric isotope patterns. A. Schauer generously helped with field work and prepared the calibration standards. A. Turnipseed, B. Backlund, and L. Scott-Denton provided additional field assistance. C. Cook, A. Schauer, M. Lott, and S. B. Bill provided mass spectrometry support. C.-T. Lai and J. Zobitz provided helpful comments on earlier versions of the manuscript, and S. Bethers helped with the graphics. This work was primarily supported by the University of Utah's Research Instrumentation Fund and other University of Utah sources. Funding for the Niwot Ridge AmeriFlux tower was provided by a grant from the South Central Section of the National Institute for Global Environmental Change through the US Department of Energy BER Program (Cooperative Agreement DE-FC03-90ER61010). We thank the University of Colorado Mountain Research Station and the Mountain Climate Program for providing weather data for the C-1 site, via funding provided by the Long-Term Ecological Research program under National Science Foundation grant DEB-9810218.

References

Allison, C. E., R. J. Francey, J. W. C. White, B. Vaughn, M. Wahlen, and A. Bollenbacher (2003), What have we learnt about stable isotope measurement from the IAEA CLASSIC?, in *Report of the Eleventh WMO/IAEA Meeting of Experts on Carbon Dioxide Concentration and Related Tracer Measurement Techniques, Tokyo, Japan*, *WMO/TD Ser.*, vol. 1138, edited by S. Toru and S. Kazuto, pp. 17–30, World Meteorol. Org., Geneva.

Aubinet, M., B. Heinesch, and M. Yernaux (2003), Horizontal and vertical CO_2 advection in a sloping forest, *Boundary Layer Meteorol.*, *108*, 397–417.

Bakwin, P. S., P. P. Tans, J. W. C. White, and R. J. Andrew (1998), Determination of the isotopic ($^{13}C/^{12}C$) discrimination by terrestrial biology from a global network of observations, *Global Biogeochem. Cycles*, *12*, 555–562.

Baldocchi, D. D., and D. R. Bowling (2003), Modelling the discrimination of $^{13}CO_2$ above and within a temperate broad-leaved forest canopy on hourly to seasonal time scales, *Plant Cell Environ.*, *26*, 231–244.

Baldocchi, D. D., and T. P. Meyers (1998), On using eco-physiological, micrometeorological and biogeochemical theory to evaluate carbon dioxide, water vapor and trace gas fluxes over vegetation: A perspective, *Agric. For. Meteorol.*, *90*, 1–25.

Baldocchi, D., et al. (2001), FLUXNET: A new tool to study the temporal and spatial variability of ecosystem-scale carbon dioxide, water vapor, and energy flux densities, *Bull. Am. Meteorol. Soc.*, *82*, 2415–2434.

Balesdent, J., C. Girardin, and A. Mariotti (1993), Site-related $\delta^{13}C$ of tree leaves and soil organic matter in a temperate forest, *Ecology*, *74*, 1713–1721.

Barford, C. C., S. C. Wofsy, M. L. Goulden, J. W. Munger, E. H. Pyle, S. P. Urbanski, L. Hutyra, S. R. Saleska, D. Fitzjarrald, and K. Moore (2001), Factors controlling long- and short-term sequestration of atmospheric CO_2 in a mid-latitude forest, *Science*, *294*, 1688–1691.

Bowling, D. R., D. D. Baldocchi, and R. K. Monson (1999), Dynamics of isotopic exchange of carbon dioxide in a Tennessee deciduous forest, *Global Biogeochem. Cycles*, *13*, 903–922.

Bowling, D. R., P. P. Tans, and R. K. Monson (2001), Partitioning net ecosystem carbon exchange with isotopic fluxes of CO_2, *Global Change Biol.*, *7*, 127–145.

Bowling, D. R., N. G. McDowell, B. J. Bond, B. E. Law, and J. R. Ehleringer (2002), ^{13}C content of ecosystem respiration is linked to precipitation and vapor pressure deficit, *Oecologia*, *131*, 113–124.

Bowling, D. R., D. E. Pataki, and J. R. Ehleringer (2003a), Critical evaluation of micrometeorological methods for measuring ecosystem-atmosphere isotopic exchange of CO_2, *Agric. For. Meteorol.*, *116*, 159–179.

Bowling, D. R., S. D. Sargent, B. D. Tanner, and J. R. Ehleringer (2003b), Tunable diode laser absorption spectroscopy for stable isotope studies of ecosystem-atmosphere CO_2 exchange, *Agric. For. Meteorol.*, *118*, 1–19.

Bowling, D. R., N. G. McDowell, J. M. Welker, B. J. Bond, B. E. Law, and J. R. Ehleringer (2003c), Oxygen isotope content of CO_2 in nocturnal ecosystem respiration: 1. Observations in forests along a precipitation transect in Oregon, USA, *Global Biogeochem. Cycles*, *17*(4), 1120, doi:10.1029/2003GB002081.

Bowling, D. R., N. G. McDowell, J. M. Welker, B. J. Bond, B. E. Law, and J. R. Ehleringer (2003d), Oxygen isotope content of CO_2 in nocturnal ecosystem respiration: 2. Short-term dynamics of foliar and soil component fluxes in an old-growth ponderosa pine forest, *Global Biogeochem. Cycles*, *17*(4), 1124, doi:10.1029/2003GB002082.

Buchmann, N., J. M. Guehl, T. S. Barigah, and J. R. Ehleringer (1997), Interseasonal comparison of CO_2 concentrations, isotopic composition, and carbon dynamics in an Amazonian rainforest (French Guiana), *Oecologia*, *110*, 120–131.

Buchmann, N., J. R. Brooks, L. B. Flanagan, and J. R. Ehleringer (1998), Carbon isotope discrimination of terrestrial ecosystems, in *Stable Isotopes: Integration of Biological, Ecological, and Geochemical Processes*, edited by H. Griffiths, pp. 203–221, BIOS Sci., Oxford, UK.

Ciais, P., P. P. Tans, M. Trolier, J. W. C. White, and R. Francey (1995), A large Northern Hemisphere terrestrial CO_2 sink indicated by the $^{13}C/^{12}C$ ratio of atmospheric CO_2, *Science*, *269*, 1098–1102.

Conway, T. J., P. P. Tans, L. S. Waterman, K. W. Thoning, D. R. Kitzis, K. A. Masarie, and N. Zhang (1994), Evidence for interannual variability of the carbon cycle from the National Oceanic and Atmospheric Administration/Climate Monitoring and Diagnostics Laboratory Global Air Sampling Network, *J. Geophys. Res.*, *99*(D11), 22,831–22,855.

Curtis, P. S., P. J. Hanson, P. Bolstad, C. Barford, J. C. Randolph, H. P. Schmid, and K. B. Wilson (2002), Biometric and eddy-covariance based estimates of annual carbon storage in five eastern North American deciduous forests, *Agric. For. Meteorol.*, *113*, 3–19.

Damesin, C., and C. LeLarge (2003), Carbon isotope composition of current-year shoots from *Fagus sylvatica* in relation to growth, respiration, and use of reserves, *Plant Cell Environ.*, *26*, 207–219.

Ehleringer, J. R., A. E. Hall, and G. D. Farquhar (1993), *Stable Isotopes and Plant Carbon-Water Relations*, Elsevier, New York.

Ekblad, A., and P. Högberg (2001), Natural abundance of ^{13}C in CO_2 respired from forest soils reveals speed of link between tree photosynthesis and root respiration, *Oecologia*, *127*, 305–308, doi:10.1007/s004420100667.

Fernandez, I., N. Mahieu, and G. Cadisch (2003), Carbon isotopic fractionation during decomposition of plant materials of different quality, *Global Biogeochem. Cycles*, *17*(3), 1075, doi:10.1029/2001GB001834.

Fessenden, J. E., and J. R. Ehleringer (2003), Temporal variation in $\delta^{13}C$ of ecosystem respiration in the Pacific Northwest: Links to moisture stress, *Oecologia*, *136*, 129–136, doi:10.1007/s00442-003-1260-1.

Fitter, A. H., G. K. Self, T. K. Brown, D. S. Bogie, J. D. Graves, D. Benham, and P. Ineson (1999), Root production and turnover in an upland grassland subjected to artificial soil warming respond to radiation flux and nutrients, not temperature, *Oecologia*, *120*, 575–581.

Flanagan, L. B., J. R. Brooks, G. T. Varney, S. C. Berry, and J. R. Ehleringer (1996), Carbon isotope discrimination during photosynthesis and the isotope ratio of respired CO_2 in boreal forest ecosystems, *Global Biogeochem. Cycles*, *10*, 629–640.

Gessler, A., S. Schrempp, A. Matzarakis, H. Mayer, H. Rennenberg, and M. A. Adams (2001), Radiation modifies the effect of water availability on the carbon isotope composition of beech (*Fagus sylvatica*), *New Phytol.*, *150*, 653–664.

Ghashghaie, J., F.-W. Badeck, G. Lanigan, S. Nogues, G. Tcherkez, E. Deleens, G. Cornic, and H. Griffiths (2003), Carbon isotope fractionation during dark respiration and photorespiration in C_3 plants, *Phytochem. Rev.*, *2*, 145–161.

Gleixner, G., H.-J. Danier, R. A. Werner, and H.-L. Schmidt (1993), Correlations between the ^{13}C content of primary and secondary plant products in different cell compartments and that in decomposing basidiomycetes, *Plant Physiol.*, *102*, 1287–1290.

Goulden, M. L., J. W. Munger, S.-M. Fan, B. C. Daube, and S. C. Wofsy (1996), Exchange of carbon dioxide by a deciduous forest: Response to interannual climate variability, *Science*, *271*, 1576–1578.

Greenland, D. (1989), The climate of Niwot Ridge, Front Range, Colorado, U.S.A., *Arct. Alpine Res.*, *21*, 380–391.

Griffis, T. J., J. M. Baker, S. D. Sargent, B. D. Tanner, and J. Zhang (2004), Measuring field-scale isotopic CO_2 fluxes with tunable diode laser absorption spectroscopy and micrometeorological techniques, *Agric. For. Meteorol.*, *124*, 15–29.

Gruber, N., C. D. Keeling, R. B. Bacastow, P. R. Guenther, T. J. Lueker, M. Wahlen, H. A. J. Meijer, W. G. Mook, and T. F. Stocker (1999), Spatiotemporal patterns of carbon-13 in the global surface oceans and the oceanic Suess effect, *Global Biogeochem. Cycles*, *13*, 307–335.

Henn, M. R., and I. H. Chapela (2000), Differential C isotope discrimination by fungi during decomposition of C_3- and C_4-derived sucrose, *Appl. Environ. Microbiol.*, *66*, 4180–4186.

Hurwitz, M. D., D. M. Ricciuto, P. S. Bakwin, K. J. Davis, W. Wang, C. Yi, and M. A. Butler (2004), Transport of carbon dioxide in the presence of storm systems over a northern Wisconsin forest, *J. Atmos. Sci.*, *61*, 607–618.

Janssens, I. A., et al. (2001), Productivity overshadows temperature in determining soil and ecosystem respiration across European forests, *Global Change Biol.*, *7*, 269–278.

Jarvis, P. G., J. M. Massheder, S. E. Hale, J. B. Moncrieff, M. Rayment, and S. L. Scott (1997), Seasonal variation of carbon dioxide, water vapor, and energy exchanges of a boreal black spruce forest, *J. Geophys. Res.*, *102*(D24), 28,953–28,966.

Keeling, C. D. (1958), The concentration and isotopic abundances of atmospheric carbon dioxide in rural areas, *Geochim. Cosmochim. Acta*, *13*, 322–334.

Keitel, C., M. A. Adams, T. Holst, A. Matzarakis, H. Mayer, H. Rennenberg, and A. Gessler (2003), Carbon and oxygen isotope composition of organic compounds in the phloem sap provides a short-term measure for stomatal conductance of European beech (*Fagus sylvatica* L.), *Plant Cell Environ.*, *26*, 1157–1168.

King, D. B., R. C. Schnell, R. M. Rosson, and C. Sweet (Eds.) (2002), *Climate Monitoring Diagnostic Laboratory Summary Report 26 2000–2001*, 184 pp., NOAA Oceanic and Atmos. Res., Boulder, Colo.

Klumpp, K., R. Schäufele, M. Lötscher, F. A. Lattanzi, W. Feneis, and H. Schnyder (2005), C-isotope composition of CO_2 respired by shoots and roots: Fractionation during dark respiration?, *Plant Cell Environ.*, *28*, 241–250.

Knohl, A. (2003), Carbon dioxide exchange and isotopic signature (^{13}C) of an unmanaged 250 year-old deciduous forest, Ph.D. dissertation, Friedrich-Schiller Univ., Jena, Germany.

Knohl, A., R. A. Werner, W. A. Brand, and N. Buchmann (2005), Short-term variations in $\delta^{13}C$ of ecosystem respiration reveals link between assimilation and respiration in a deciduous forest, *Oecologia*, *142*, 70–82.

Lai, C.-T., A. J. Schauer, C. Owensby, J. M. Ham, and J. R. Ehleringer (2003), Isotopic air sampling in a tallgrass prairie to partition net ecosystem CO_2 exchange, *J. Geophys. Res.*, *108*(D18), 4566, doi:10.1029/2002JD003369.

Lai, C.-T., J. R. Ehleringer, P. Tans, S. C. Wofsy, S. P. Urbanski, and D. Y. Hollinger (2004), Estimating photosynthetic ^{13}C discrimination in terrestrial CO_2 exchange from canopy to regional scales, *Global Biogeochem. Cycles*, *18*, GB1041, doi:10.1029/2003GB002148.

Lai, C-.T., J. R. Ehleringer, A. J. Schauer, P. P. Tans, D. Y. Hollinger, K. T. Paw U, J. W. Munger, and S. C. Wofsy (2005), Canopy-scale $\delta^{13}C$ of

photosynthetic and respiratory CO_2 fluxes: Observations in forest biomes across the United States, *Global Change Biol.*, *11*, 1–11.

Law, B. E., M. G. Ryan, and P. M. Anthoni (1999), Seasonal and annual respiration of a ponderosa pine ecosystem, *Global Change Biol.*, *5*, 169–182.

Law, B. E., et al. (2002), Environmental controls over carbon dioxide and water vapor exchange of terrestrial vegetation, *Agric. For. Meteorol.*, *113*, 97–120.

Lloyd, J., et al. (1996), Vegetation effects on the isotopic composition of atmospheric CO_2 at local and regional scales: Theoretical aspects and a comparison between rain forest in Amazonia and a boreal forest in Siberia, *Aust. J. Plant Physiol.*, *23*, 371–399.

McDowell, N. G., D. R. Bowling, A. Schauer, J. Irvine, B. J. Bond, B. E. Law, and J. R. Ehleringer (2004), Associations between carbon isotope ratios of ecosystem respiration, water availability and canopy conductance, *Global Change Biol.*, *10*, 1767–1784, doi:10.1111/j.1365-2486.2004.00837.x.

Mencuccini, M., J. Grace, J. Moncrieff, and K. G. McNaughton (Eds.) (2004), *Forests at the Land-Atmosphere Interface*, CABI Publ., Wallingford, UK.

Miller, J. B., and P. P. Tans (2003), Calculating isotopic fractionation from atmospheric measurements at various scales, *Tellus, Ser. B*, *55*, 207–214.

Miller, J. B., P. P. Tans, J. W. C. White, T. J. Conway, and B. Vaughn (2003), The atmospheric signal of terrestrial carbon isotopic discrimination and its implication for partitioning carbon fluxes, *Tellus, Ser. B*, *55*, 197–206.

Monson, R. K., A. A. Turnipseed, J. P. Sparks, P. C. Harley, L. E. Scott-Denton, K. Sparks, and T. E. Huxman (2002), Carbon sequestration in a high-elevation, subalpine forest, *Global Change Biol.*, *8*, 459–478.

Mortazavi, B., J. P. Chanton, J. L. Prater, A. C. Oishi, R. Oren, and G. Katul (2005), Temporal variability in ^{13}C of respired CO_2 in a pine and a hardwood forest subject to similar climatic conditions, *Oecologia*, *142*, 57–69.

Ogée, J., P. Peylin, P. Ciais, T. Bariac, Y. Brunet, P. Berbigier, C. Roche, P. Richard, G. Bardoux, and J.-M. Bonneford (2003), Partitioning net ecosystem carbon exchange into net assimilation and respiration using $^{13}CO_2$ measurements: A cost-effective sampling strategy, *Global Biogeochem. Cycles*, *17*(2), 1070, doi:10.1029/2002GB001995.

Ogée, J., P. Peylin, M. Cuntz, T. Bariac, Y. Brunet, P. Berbigier, P. Richard, and P. Ciais (2004), Partitioning net ecosystem carbon exchange into net assimilation and respiration with canopy-scale isotopic measurements: an error propagation analysis with $^{13}CO_2$ and $CO^{18}O$ data, *Global Biogeochem. Cycles*, *18*, GB2019, doi:10.1029/2003GB002166.

Parrish, D. D., et al. (1990), Systematic variations in the concentration of NO_x (NO plus NO_2) at Niwot Ridge, Colorado, *J. Geophys. Res.*, *95*(D2), 1817–1836.

Parrish, D. D., M. Trainer, M. P. Buhr, B. A. Watkins, and F. C. Fehsenfeld (1991), Carbon monoxide concentrations and their relation to concentrations of total reactive oxidized nitrogen at two rural U.S. sites, *J. Geophys. Res.*, *96*(D5), 9309–9320.

Pataki, D. E., J. R. Ehleringer, L. B. Flanagan, D. Yakir, D. R. Bowling, C. J. Still, N. Buchmann, J. O. Kaplan, and J. A. Berry (2003), The application and interpretation of Keeling plots in terrestrial carbon cycle research, *Global Biogeochem. Cycles*, *17*(1), 1022, doi:10.1029/2001GB001850.

Pate, J., and D. Arthur (1998), $\delta^{13}C$ analysis of phloem sap carbon: Novel means of evaluating seasonal water stress and interpreting carbon isotope signatures of foliage and trunk wood of *Eucalyptus globulus*, *Oecologia*, *117*, 301–311.

Quay, P., R. Sonnerup, T. Westby, J. Stutsman, and A. McNichol (2003), Changes in the $^{13}C/^{12}C$ of dissolved inorganic carbon in the ocean as a tracer of anthropogenic CO_2 uptake, *Global Biogeochem. Cycles*, *17*(1), 1004, doi:10.1029/2001GB001817.

Randerson, J. T., G. J. Collatz, J. E. Fessenden, A. D. Munoz, C. J. Still, J. A. Berry, I. Y. Fung, N. Suits, and A. S. Denning (2002), A possible global covariance between terrestrial gross primary production and ^{13}C discrimination: Consequences for the atmospheric ^{13}C budget and its response to ENSO, *Global Biogeochem. Cycles*, *16*(4), 1136, doi:10.1029/2001GB001845.

Raupach, M. R. (2001), Inferring biogeochemical sources and sinks from atmospheric concentrations: General considerations and applications in vegetation canopies, in *Global Biogeochemical Cycles in the Climate System*, edited by E.-D. Schulze et al., 41–59, Elsevier, New York.

Santruckova, H., M. I. Bird, and J. Lloyd (2000), Microbial processes and carbon-isotope fractionation in tropical and temperate grassland soils, *Funct. Ecol.*, *14*, 108–114.

Schimel, D., T. G. F. Kittel, S. Running, R. Monson, A. Turnipseed, and D. Anderson (2002), Carbon sequestration studied in western U. S. mountains, *EOS Trans. AGU*, *83*, 445–449.

Schmid, H.-P. (1997), Experimental design for flux measurements: Matching scales of observations and fluxes, *Agric. For. Meteorol.*, *87*, 179–200.

Schnyder, H., R. Schäufele, M. Lötscher, and T. Gebbing (2003), Disentangling CO_2 fluxes: Direct measurements of mesocosm-scale natural abundance $^{13}CO_2/^{12}CO_2$ gas exchange, ^{13}C discrimination, and labeling of CO_2 exchange flux components in controlled environments, *Plant Cell Environ.*, *26*, 1863–1874.

Scholze, M., J. O. Kaplan, W. Knorr, and M. Heimann (2003), Climate and interannual variability of the atmosphere-biosphere $^{13}CO_2$ flux, *Geophys. Res. Lett.*, *30*(2), 1097, doi:10.1029/2002GL015631.

Staebler, R. M., and D. R. Fitzjarrald (2004), Observing subcanopy CO_2 advections, *Agric. For. Meteorol.*, *122*, 139–156.

Sternberg, L. S. L. (1989), A model to estimate carbon dioxide recycling in forests using $^{13}C/^{12}C$ ratios and concentrations of ambient carbon dioxide, *Agric. For. Meteorol.*, *48*, 163–173.

Thoning, K. W., T. J. Conway, N. Zhang, and D. Kitzis (1995), Analysis system for measurement of CO_2 mixing ratios in flask air samples, *J. Atmos. Oceanic Technol.*, *12*, 1349–1356.

Trolier, M., J. W. C. White, P. P. Tans, K. A. Masarie, and P. A. Gemery (1996), Monitoring the isotopic composition of atmospheric CO_2: Measurements from the NOAA Global Air Sampling Network, *J. Geophys. Res.*, *101*(D20), 25,897–25,916.

Turnipseed, A. A., P. D. Blanken, D. E. Anderson, and R. K. Monson (2002), Energy budget above a high-elevation subalpine forest in complex topography, *Agric. For. Meteorol.*, *110*, 177–201.

Turnipseed, A. A., D. E. Anderson, P. D. Blanken, W. M. Baugh, and R. K. Monson (2003), Airflows and turbulent flux measurements in mountainous terrain: Part 1. Canopy and local effects, *Agric. For. Meteorol.*, *119*, 1–21.

Turnipseed, A. A., D. E. Anderson, S. P. Burns, P. D. Blanken, and R. K. Monson (2004), Airflows and turbulent flux measurements in mountainous terrain: Part 2: Mesoscale effects, *Agric. For. Meteorol.*, *125*, 187–205.

Valentini, R. (Ed.) (2003), *Fluxes of Carbon, Water, and Energy of European Forests*, Springer, New York.

Valentini, R., et al. (2000), Respiration as the main determinant of carbon balance in European forests, *Nature*, *404*, 861–865.

van Dijk, A. I. J. M., and A. J. Dolman (2004), Estimates of CO_2 uptake and release among European forests based on eddy covariance data, *Global Change Biol.*, *10*, 1445–1459.

Yakir, D., and X.-F. Wang (1996), Fluxes of CO_2 and water between terrestrial vegetation and the atmosphere estimated from isotope measurements, *Nature*, *380*, 515–517.

Yi, C., K. J. Davis, P. S. Bakwin, B. W. Berger, and L. C. Marr (2000), Influence of advection on measurements of the net ecosystem-atmosphere exchange of CO_2 from a very tall tower, *J. Geophys. Res.*, *105*(D8), 9991–9999.

Yi, C., et al. (2004), A nonparametric method for separating photosynthesis and respiration components in CO_2 flux measurements, *Geophys. Res. Lett.*, *31*, L17107, doi:10.1029/2004GL020490.

D. R. Bowling, Department of Biology, 257 South 1400 East, University of Utah, Salt Lake City, UT 84112-0820, USA. (bowling@biology.utah.edu)

S. P. Burns, Department of Ecology and Evolutionary Biology, University of Colorado, Boulder, CO 80309, USA. (sean.burns@colorado.edu)

T. J. Conway, NOAA Climate Monitoring and Diagnostics Laboratory, 325 Broadway, Boulder, CO 80305, USA. (thomas.j.conway@noaa.gov)

R. K. Monson, Cooperative Institute for Research in Environmental Science, University of Colorado, Boulder, CO 80309, USA. (monsonr@colorado.edu)

J. W. C. White, Institute of Arctic and Alpine Research (INSTAAR), Campus Box 450, University of Colorado, Boulder, CO 80309, USA. (jwhite@colorado.edu)